Published in final edited form as:
Sens Actuators B Chem. 2011 December 15; 160(1): 1363–1371. doi:10.1016/j.snb.2011.09.079.

Thermodynamic Analysis of the Selectivity Enhancement Obtained by Using Smart Hydrogels That Are Zwitterionic When Detecting Glucose With Boronic Acid Moieties

F. Horkay[a,*], **S. H. Cho**[b], **P. Tathireddy**[c], **L. Rieth**[c], **F. Solzbacher**[c,d,e], and **J. Magda**[b,d,+]

[a]Section on Tissue Biophysics and Biomimetics, Program on Pediatric Imaging and Tissue Sciences, Eunice Kennedy Shriver National Institute of Child Health and Human Development, National Institutes of Health, Bethesda, MD 20892-5772 USA

[b]Department of Chemical Engineering, University of Utah, Salt Lake City, Utah 84112 USA

[c]Department of Electrical & Computer Engineering, University of Utah, Salt Lake City, Utah 84112 USA

[d]Department of Materials Science & Engineering, University of Utah, Salt Lake City, Utah 84112 USA

[e]Department of Bioengineering, University of Utah, Salt Lake City, Utah 84112 USA

Abstract

Because the boronic acid moiety reversibly binds to sugar molecules and has low cytotoxicity, boronic acid-containing hydrogels are being used in a variety of implantable glucose sensors under development, including sensors based on optical, fluorescence, and swelling pressure measurements. However, some method of glucose selectivity enhancement is often necessary, because isolated boronic acid molecules have a binding constant with glucose that is some forty times smaller than their binding constant with fructose, the second most abundant sugar in the human body. In many cases, glucose selectivity enhancement is obtained by incorporating pendant tertiary amines into the hydrogel network, thereby giving rise to a hydrogel that is *zwitterionic* at physiological pH. However, the mechanism by which incorporation of tertiary amines confers selectivity enhancement is poorly understood. In order to clarify this mechanism, we use the osmotic deswelling technique to compare the thermodynamic interactions of glucose and fructose with a zwitterionic smart hydrogel containing boronic acid moieties. We also investigate the change in the structure of the hydrogel that occurs when it binds to glucose or to fructose using the technique of small angle neutron scattering.

[*]Corresponding Author. Telephone (301) 435-7229, Fax (301) 435-5035, horkay@helix.nih.gov. [+]Corresponding Author. Telephone (801) 581-7536, Fax (801) 585-9291, jj.magda@utah.edu.

Disclosure Statement

For full disclosure and conflict-of-interest transparency, it should be noted that J. Magda, F. Solzbacher, and P. Tathireddy have financial interests in an early-stage startup company (pre-IPO) located in Salt Lake City, Utah (Blackrock Sensors, Inc.) that is licensing hydrogel-based sensing technology.

Keywords

glucose sensor; smart hydrogel; boronic acid; monosaccharides; SANS

1. Introduction

The development of novel glucose sensors continues to be one the most widely studied areas of sensor research, due to the continuing need for improvements in glucose sensors used in the management of diabetes [1–2] and in control of fermentation processes [3–4]. The first type of continuous glucose sensor developed over twenty years ago was an amperometric electrochemical glucose sensor that used the enzyme *glucose oxidase* (GOx) for glucose recognition [5–6]. This type of glucose sensor is relatively fast and small, and research on improvements to amperometric glucose sensors continues unabated [7–9]. However, even though GOx is highly specific to glucose, the use of GOx as a recognition element for glucose suffers from the following disadvantages: (1) the enzyme GOx is susceptible to denaturation with subsequent loss of activity; (2) GOx requires oxygen or another redox mediator and is thus unsuitable for anaerobic fermentation reactors [4], (3) the reaction catalyzed by GOx continuously consumes the analyte (glucose) and produces a potentially harmful by-product (H_20_2). This last point implies that sensors employing GOx are transport sensors rather than equilibrium sensors, with sensitivities that vary with the glucose diffusion coefficient. For these reasons, many of the newer glucose sensors under development use the boronic acid moiety rather than GOx as the recognition element for glucose [10–27]. This includes sensors based on optical [11–14,16,18,20–21,27], fluorescence [25–26], surface plasmon [23], and swelling pressure measurements [17,24]. Small molecules containing boronic acid have been known for over a century to strongly yet reversibly bind cis-diols on glucose and other monosaccharides to give cyclic boronic acid esters in aqueous media [28], as shown schematically in Figure 1. Kataoka and co-workers appear to be the first research group to incorporate boronic acid moieties into smart hydrogels, thereby obtaining “totally synthetic” polymer gels that reversibly swell in response to increases in the environmental glucose concentration [29]. At physiological pH (7.4), this hydrogel is a slightly charged poly(anion), because the pKa value for isolated boronic acid groups is about 8.86 [30]. Unfortunately, this smart hydrogel and others of similar chemistry are actually more responsive to fructose than to glucose. This is not surprising, because small molecule spectroscopic studies show that the isolated boronic acid moiety has a binding constant with fructose that is about forty times greater than its binding constant with glucose [28]. Thus, even though the normal physiological concentration of fructose is approximately 200 times smaller than that of glucose [31], some method of glucose selectivity enhancement is thought to be necessary. In the last ten years, a number of research groups working on a variety of different types of glucose sensors have determined that beneficial effects can be obtained by using zwitterionic polymers or zwitterionic hydrogels obtained by incorporating pendant tertiary amines into the polymers or hydrogels nearby to the boronic acid moities [12,14,18,20–21,24,27,30,32]. The chosen tertiary amines are Lewis bases that accept a proton to become cations at physiological pH. In addition, for polymers at least, the incorporation of tertiary amines facilitates the ionization of nearby boronic acid groups [33]. As an example of the benefits to glucose selectivity of this approach, consider the results of Horgan et al., who developed a holographic glucose sensor in which a diffraction grating is embedded within a glucose-responsive hydrogel [14]. The signal from this sensor is the measured change in the wavelength of diffracted light in response to an increase in the concentration of environmental glucose or fructose concentration from zero to 5.7 mM, the normal glucose physiological value. When the holographic sensor was used with a smart hydrogel containing boronic acid but no tertiary amines, the optical response observed was a red shift of 761 nm for fructose, and a red shift

of 40 nm for glucose. On the other hand, when the holographic sensor was used with a smart hydrogel containing an equimolar ratio of boronic acid and tertiary amine, the optical response observed was a red shift of only 13 nm for fructose, and a *blue shift* of 50 nm for glucose. The results of Horgan et al. are indicative of the two trends that have been observed by a number of different research groups [12,14,18,20–21,24,27,32] when tertiary amines are incorporated into glucose-responsive hydrogels containing boronic acid moieties: (1) an increase in the magnitude of hydrogel glucose response relative to the magnitude of the fructose or lactate response, and (2) a change in the *direction* of the hydrogel response to an increase in glucose concentration from swelling to shrinking. A thermodynamic model based on reversible cross-linking proposed by Alexeev et al [12] that explains both of these trends has become widely accepted by other researchers in the field [14,18,20–21,24,27,32]. According to Alexeev et al. [12], glucose is relatively unique among monosaccharides in that it can bind simultaneously to two different boronic acid moieties, thereby forming reversible glucose-bis(boronate) cross-links in the hydrogel network. The associated thermodynamic model further assumes that the free energy of mixing (Π_{mix}) of glucose with the hydrogel is negligible implying that all glucose molecules bind onto the boronic acid groups and do not influence the thermodynamic interactions between the polymer and the solvent, and thus the glucose response of the zwitterionic smart hydrogel arises *solely* from the formation or breakage of glucose-mediated cross-links [12]. However, as far as we know, there is of yet no direct spectroscopic evidence that glucose-bis(boronate) cross-links form in hydrogels, though NMR studies on small organic molecules show that *both* glucose and fructose can simultaneously bind to two boronic acid groups [28]. We do not dispute the importance of glucose-mediated cross-links, but feel it is necessary in the following to re-examine the additional assumption that the change in the free energy of mixing (Π_{mix}) does not contribute significantly to zwitterionic hydrogel glucose response. To investigate the effect of glucose on the thermodynamic properties of these gels it is important to separate the elastic and mixing free energy components. To this end we made osmotic swelling pressure measurements on gels containing relatively low amounts (8 mole %) of boronic acid moieties. The low boronic acid content reduces the number of additional cross-links formed in the presence of glucose.

2. Thermodynamics

Unconfined neutral hydrogels swell until the total change in free energy, ΔF_{tot}, reaches a minimum or, equivalently, until the chemical potential of each mobile species becomes equal in the coexisting phases. The mixing of water with the polymer chains makes a negative contribution to the free energy (ΔF_{mix}), while the stretching of the hydrogel network makes a positive contribution (ΔF_{el}). Assuming these terms are independent, we can write [12, 34–36]:

$$\Delta F_{tot} = \Delta F_{mix} + \Delta F_{el} \quad (1)$$

In the case of charged hydrogels, the ions also contribute to ΔF_{tot}. However, at high ionic strength (0.16 M), the ionic contribution can be neglected [12], as shown by several experimental studies on highly swollen polyelectrolyte hydrogels (e.g., polyacrylic acid gels, DNA gels) [36–37] as well as molecular dynamics simulations [38].

In an osmotic swelling experiment the measurable quantities involve derivatives of the free energy, i.e.

$$\Pi_{tot} = -\frac{1}{V_1}\left(\frac{\partial \Delta F_{tot}}{\partial n_1}\right) = \Pi_{mix} + \Pi_{el} \tag{2}$$

where Π_{tot} is the swelling pressure of the gel, Π_{mix} and Π_{el} are the mixing and elastic contributions of Π_{tot}, respectively, V_1 is the molar volume of solvent (water), and n_1 is the number of moles of water. At swelling equilibrium with the pure solvent Π_{tot} must equal zero. One can study nonzero values of the total swelling pressure by equilibrating the hydrogel with an osmotic stressing agent of known osmotic pressure [36–37], or by squeezing the water out of the hydrogel using a known mechanical (hydrostatic) pressure [39].

According to a Flory-Huggins type equation, Π_{mix} is given by:

$$\Pi_{mix} = -\frac{RT}{V_1}[\ln C + C + \chi_0 C^2 + \chi_1 C^3] \tag{3},$$

where C is the weight fraction of the polymer in the hydrogel, χ_0 and χ_1 are the Flory-Huggins parameters for binary and ternary interactions, respectively, between the polymer network and the solution, R is the gas constant, and T is the temperature. The elastic contribution Π_{el} is given by [12, 36]:

$$\Pi_{el} = -\frac{RTn_{cr}}{V_m}\left[\left(\frac{V_m}{V}\right)^{1/3} - \frac{1}{2}\left(\frac{V_m}{V}\right)\right] = -G \tag{4},$$

where V_m is the volume of the relaxed network, n_{cr} is effective number of cross-linked chains in the network, and G is network elastic shear modulus. In their analysis of zwitterionic glucose-responsive hydrogels, the main assumption of Alexeev et al. [12] is that the hydrogel glucose response is dominated by the increase in n_{cr} with increase in glucose concentration; i.e. $|\Delta\Pi_{el}| >> \Delta\Pi_{mix}$ for an increase in glucose concentration within the range of physiological interest (0 – 20 mM). It is this assumption that we check in the following sections.

3. Experimental Methods

3.1 Materials

The monomers used for preparation of the gels were obtained as follows: acrylamide (AAM, Fisher Scientific), *N*,*N*-methylenebisacrylamide (BIS, Sigma-Aldrich), 3-acrylamidophenylboronic acid (3-APB, Frontier Scientific, Logan, UT), and N-(3-dimethylaminopropyl acrylamide (DMAPAA). The monomers were used as received. Ammonium peroxydisulfate (APS, Sigma-Aldrich), N,N,N',N'-tetramethylethylenediamine (TEMED, Sigma-Aldrich), 2,2-dimethoxy-2-phenylacetophenone (Sigma-Aldrich), 1-vinyl-2-pyrrolidinone (Sigma-Aldrich), D(+)-glucose (Mallinckrodt Chemicals), D(−)-fructose (Sigma-Aldrich), dimethyl sulfoxide (DMSO, Sigma-Aldrich), 4-(2-Hydroxyethyl)piperazine-1-ethanesulfonic acid (HEPES,Sigma-Aldrich), and Dulbecco's phosphate-buffered saline solution (1X PBS, Sigma-Aldrich) were also used as received. Market grade wire cloth mesh (type 304 stainless steel, 80 mesh, wire opening 178 μm, open area 31%) was obtained from Small Parts, Inc., Miramar, FL, USA.

3.2 Hydrogel Synthesis

Zwitterionic glucose-sensitive hydrogels (GSHs) containing AAM/3-APB/DMAPAA/BIS at a nominal mole ratio of 80/8/10/2 were prepared by free radical cross-linking copolymerization. This is the same composition previously studied by Tierney et al. [20–21] and Lin et al. [24]. GSHs were prepared in molds of three different thickness values: 0.4 mm for samples used in glucose sensor tests, 1 mm for samples used for osmotic swelling pressure and SANS measurements, and 5 mm for samples used for shear modulus measurements. Samples 0.4 mm and 1 mm thick were prepared by either thermal or UV curing, whereas only thermal curing was used to prepare samples 5 mm thick. (In thicker samples UV curing does not result in homogeneous gels.) The polymer concentration in the pre-gel solution prior to curing was 13 wt.%, or 20 wt% in a few selected cases. In brief, stock solutions were prepared of AAM and BIS in 1 mM HEPES buffer. Appropriate amounts of the two stock solutions were mixed in a vial with DMAPAA and TEMED in the case of thermal curing. In order to dissolve 3-APB into the pregel solution, 10 vol% of DMSO was added into the vial. In thermal curing, the free radical initiator APS was introduced after purging the vial with N_2 gas for ten minutes, after which the pre-gel solution was rapidly injected into a cavity between two square plates (polycarbonate and poly(methyl methacrylate)) of surface area 60 cm^2. After approximately 12 hours of reaction at room temperature, the hydrogel slab was removed from the mold and washed for at least two days with deionized water and 1X PBS buffer (pH 7.4, ionic strength 0.16 M) before testing. For UV curing, the photoinitator combination 2,2-dimethoxy-2-phenylacetophenone/1-vinyl-2-pyrrolidinone was used instead of the thermal initiator combination TEMED/APS. After purging with N_2 gas for ten minutes, the pre-gel solution was injected into a cavity of known thickness between a glass plate and a poly(methacrylate) plate.

Photopolymerization was induced by exposing the pre-gel solution through the glass plate to UV light (365 nm, 10 mW/cm^2) for 2.5 min. The GSHs obtained were first washed with DI water for about one day and then stored in 1X PBS buffer. The samples were also subjected to two cycles of ionic strength change between 0.16 M and 0.05M PBS in order to further clean the hydrogels. The hydrogels were stored in 0.16 M PBS until testing. Prior to SANS measurements, the water in the hydrogel was exchanged with D_2O as described below. The solvent exchange did not cause appreciable change in the swelling degree. In order to estimate the water content, GSH samples were dried in an oven at 50 °C with the weight monitored as a function of time. A GSH sample synthesized in 1 mM HEPES buffer at 13 wt.% polymer and equilibrated with 1X PBS at pH 7.4 was shown to contain on average 88 wt% water. A GSH sample synthesized in 1 mM HEPES buffer at 20 wt.% polymer and equilibrated with 1X PBS at pH 7.4 was shown to contain on average 85 wt% water.

3.3 Sugar Sensor Construction and Sensor Response Tests

As analyzed in detail in recent publications in this journal [24,40], the total osmotic swelling pressure Π_{tot} of a smart hydrogel can be obtained by confining it between a porous membrane and the diaphragm of a miniature pressure transducer. In such a sensing scheme, a change in the environmental glucose concentration, as sensed through the pores of the membrane, changes Π_{tot} (see Equation 2) which must at equilibrium equal the mechanical pressure measured by the pressure transducer. Figure 2 shows a sketch of the chemomechanical sensor that was used. The sensor consists of a piezoresistive pressure transducer (model EPX-N01-0.35B, MEAS France, Les Clayes-Sous-Bois, France) with a cylindrical stainless steel sensing area (diameter 3.5 mm) completely covered with a hydrogel film of thickness ≈ 400 μm. The hydrogel is held in place in the sensor by a cap with a top surface that consists of a replaceable porous membrane through which mass transfer can occur. In keeping with the results obtained from our previous work [40], a

stainless steel wire cloth mesh (mesh size 80, wire opening 174 μm, 31 % open area) was used as the porous membrane. A GSH was synthesized and cleaned as described above, a circular biopsy tool was used to cut a disc-shaped sample of appropriate diameter, and the sample was then transferred from sugar-free PBS buffer (pH 7.4, ionic strength 0.16 M) to the sensing surface of the pressure transducer using tweezers. The sensor cap with wire mesh was attached to the sensor base by tightening three screws that were adjusted to impose an axial compressive stress on the hydrogel in the sensor. The sensor was then inserted into a large covered environmental bath containing PBS buffer at room temperature and physiological pH and ionic strength. This bath also contained a magnetic stirrer used to minimize external mass transfer resistance to the sensor. Sensor response tests were performed by either injecting solutions of glucose or fructose into the environmental bath and then noting the time-dependent response of the pressure transducer, or by rapidly switching the sensor into another environmental bath at the same ionic strength and pH but with no sugar. The time-dependent pressure signal was captured with an Agilent data acquisition system.

3.4 Total Osmotic Swelling Pressure (Π_{tot}) Measurements

The reference environmental solution (infinite bath) was chosen to be phosphate-buffered saline (PBS) solution at 25 °C with ionic strength 0.16 M and pH = 7.4. In some cases, the environmental solution also contained 5 mM glucose or 5 mM fructose. Hydrogels of known dry mass m_d were equilibrated with this reference solution, at which point gel swelling pressure Π_{tot} must equal zero. Deswelling of the gels was achieved by enclosing them in a semipermeable membrane (dialysis bag, seamless cellulose tubing; cut off molecular weight: 12 kDa, Sigma Chemical Co., St. Louis, MO). Known concentrations of an osmotic deswelling agent [poly(vinyl pyrrolidone), PVP, M_n = 29 kDa] were added to the environmental solution, and equilibrated with the gel for 8 – 10 days. The semipermeable membrane prevented penetration of PVP into the gel. At equilibrium, the swelling pressure Π_{tot} of the gel inside the dialysis bag is equal to the known osmotic pressure of the PVP solution outside [41]. Periodically the mass of the gel m_g was measured, and used to calculate the total polymer weight fraction $C = m_d/m_g$ (where m_d is the mass of the dry polymer), with hydrogel swelling ratio $Q \approx 1/C$. Equilibrium was achieved when no further changes in either gel swelling degree or solution composition were detectable. The gels samples were dried at 95 °C. First, the mass of the salt-containing gel was measured. Then the gel was soaked in large excess of distilled water to remove the salt. The swelling ratio was calculated by correcting the measured mass with the known amount of salt.

Reversibility was checked by transferring gels into PVP solutions at different osmotic pressure values.

3.5 Elastic (Shear) Modulus Measurements

Shear modulus data of fully gelled materials were obtained from uniaxial compression measurements using a TA.XT2I HR Texture Analyser (Stable Micro Systems, UK). As discussed in a standard rubber testing handbook [42], torsional measurements of the shear modulus G of fully-gelled polymers will be erroneous if sample “slip” occurs at the interface between the solid polymer and the steel rheometer plates, because then the true value of the shear strain exerted on the sample will be unknown. Hence the standard rubber testing handbook recommends lubricating the sample interface to ensure that sample slip does occur, and then determining G in the absence of “barrel” distortion by measuring the force needed to apply compressive strains (uniaxial) on the sample [42].

Equilibrated gel samples were rapidly transferred from the dialysis bag into the TA XT21 HR apparatus, which measures the compressive deformation (precision: ± 0.001 mm) as a

function of an applied force (precision: ± 0.01 N). Stress-strain isotherms were determined at 25 °C in about 3–5 minutes with no detectable change in gel weight. The absence of sample volume change and barrel distortion was confirmed, and stress-strain isotherms were found to fit the Mooney-Rivlin relation [35, 43–44]

$$\sigma = C_1(\Lambda - \Lambda^{-2}) + C_2(1 - \Lambda^{-3}) \quad (5),$$

where σ is the nominal stress (related to the undeformed cross-section of the gel), Λ is the deformation ratio ($\Lambda = L/L_o$, L and L_o are the lengths of the deformed and undeformed specimen, respectively), and C_1 an C_2 are constants. The stress-strain data were determined in the range of deformation ratio $0.7 < \Lambda < 1.0$. The value of C_2 proved to be negligibly small for the gel systems studied. In this situation, the constant C_1 can be identified with the shear modulus (G) of the swollen network.

The swelling and mechanical measurements were carried out at 25 ± 0.1 °C. Repeated measurements showed a mean change in the osmotic swelling pressure and elastic modulus less than 2–3 %.

3.6 Hydrogel Swelling Ratio Measurements as a Function of Temperature

A given hydrogel sample was immersed in a large stirred temperature-controlled vessel containing either sugar-free PBS buffer (pH 7.4, ionic strength 0.16 M), PBS buffer plus 5 mM glucose, or PBS buffer plus 5 mM fructose. Periodically, the gel sample was withdrawn from the solution and weighed after removal of excess surface solution by light blotting with a laboratory tissue. The change in relative swelling ratio for a gel sample subjected to a given change in temperature was calculated as $(m_f - m_0)/m_0$, where m_f is the mass at the final temperature, and m_0 is the mass at the initial temperature. Swelling ratio changes were measured for 3–4 small samples taken from the same reaction mold, and the standard deviation was taken as an estimate of the uncertainty in the measured swelling ratio.

3.7 Small-angle Neutron Scattering

SANS measurements were made on gels on the NG3 30 m instrument [45] at the National Institute of Standards and Technology (NIST, Gaithersburg MD). Gel samples were swollen in solutions of heavy water in 2 mm thick sample cells. The sample cell consisted of 1 mm thick quartz windows separated by a 2 mm thick spacer. The beam diameter was 20 mm. The measurements were made at three sample-detector distances, 1.3 m, 4 m and 13.1 m, with incident wavelength 8Å. The explored wave vector range was $0.003\ Å^{-1} \leq q \leq 0.2\ Å^{-1}$, and counting times from twenty minutes to two hours were used. The total counts of neutron at the detector varied in the range 0.5–3 million. After radial averaging, corrections for detector response and cell window scattering were applied. The neutron scattering intensities were calibrated using NIST absolute intensity standards. The incoherent background was subtracted following the procedure described in reference 46. All SANS experiments were carried out at 25 ± 0.1°C.

4. Results

4.1 Sugar Sensor Response Results

Figure 3 shows the response of the chemomechanical sensor (Figure 2) at 25 °C to cyclic changes in the environmental glucose concentration between zero and 5 mM at fixed pH (7.4) and fixed ionic strength (0.16 M). The response of the same sensor under the same conditions to cyclic changes in environmental fructose concentration between zero and 5 mM is shown in Figure 4. In both cases, the GSH in the sensor was prepared by thermal

curing a pre-gel solution containing 13.0 wt.% polymer in a mold of thickness 400 μm. In Figure 3, the measured value of Π_{tot} *decreases* in response to the increase in glucose concentration from zero to 5 mM. Note that 5 mM is approximately the normal blood glucose concentration in humans. The average magnitude of the decrease is 9.1 kPa ± 0.05 kPa. The response time in the macrosensor is quite large, but we have already demonstrated elsewhere a response time of order ten minutes using the same GSH in a microchip glucose sensor [47]. In Figure 4, the measured value of Π_{tot} *increases* in response to the increase in fructose concentration from zero to 5 mM. The average magnitude of the increase is 5.6 kPa ± 0.2 kPa. Note that the sensor fructose response magnitude in Figure 4 is smaller than the sensor glucose response magnitude in Figure 3, even though we introduced a fructose concentration some 200 times larger than the normal human blood value [31]. Thus when monitoring blood glucose concentration, one can safely neglect fructose interference under most conditions using the GSH of Figures 3 and 4. In addition, Tierney and co-workers have demonstrated using an optical sensor with the same GSH for glucose recognition that potential interference from physiological concentrations of lactate is negligible, and that the glucose response is essentially the same in human blood plasma as in PBS buffer, provided that the blood plasma does not contain added heparin for anti-coagulation [21].

This GSH contains both boronic acid moieties (≈ 8 mol% 3-APB) and pendant tertiary amines (≈10 mol% DMAPAA). As shown elsewhere [14,20,24,32], in the absence of pendant tertiary amines, a similar GSH would swell rather than shrink in response to an increase in glucose concentration, with a magnitude considerably less than the magnitude of the fructose swelling response. Thus the incorporation of a relatively small mole fraction of tertiary amines into the hydrogel is sufficient to dramatically enhance glucose selectivity, as noted by numerous other researchers (see Introduction).

It is also important to note that the kinetics of the swelling and shrinking process, which governs the response time of gel biosensors to changes in glucose concentration, strongly depends on the size and geometry of the sample. Fast responses can be obtained by miniaturizing the system. Furthermore, the properties of the network polymer (e.g., chemical quality and distribution of monomers, cross-link density, amounts of charged groups) also influence the dynamic properties.

4.2 Osmotic Swelling Pressure and Elastic Shear Modulus Results

The results of the osmotic deswelling experiments are shown in Figure 5 where the swelling pressure Π_{tot} of the zwitterionic GSHs is plotted against the polymer weight fraction C, in three different solvents: sugar-free PBS buffer (1X), PBS buffer plus 5 mM added glucose, and PBS buffer plus 5 mM added fructose. It is apparent that the GSH deswells when it is subjected to a given osmotic stress exerted by the PVP solution as described in Section 3.4. The amount of water retained by the GSH has its least value when placed in the glucose solution, and has its greatest value when placed in the fructose solution. The results obtained in sugar-free PBS are intermediate between the results obtained in the fructose and glucose solutions, but closer to the fructose solution results. This is consistent with the sensor results (Figures 3–4), which show that the GSH exhibits a greater change when transferred from 1X PBS buffer to the 5 mM glucose solution than to the 5 mM fructose solution. One also observes in Figure 5 that the Π_{tot} value of the zwitterionic GSH exhibits a much steeper increase with increasing polymer weight fraction in the fructose solution. This implies that *osmotic modulus* $\left[=C\left(\frac{\partial \Pi_{tot}}{\partial C}\right)_T\right]$ of the GSH, its resistance to having its water content reduced by compression, is larger in the fructose solution.

Combining Equations (2) – (4), one obtains the Flory-Huggins theoretical prediction for the results of Figure 5:

$$\Pi_{tot}=\Pi_{mix}+\Pi_{el}=-\frac{RT}{V_1}[\ln C+C+\chi_0 C^2+\chi_1 C^3]-G \quad (6),$$

According to Equation (6), Π_{tot} is the sum of a mixing contribution Π_{mix} and an elastic contribution Π_{el}, where the elastic contribution is taken to be the negative of the shear modulus G [36]. The value of G was independently measured as a function of polymer weight fraction in the same three solutions (see Experimental). Figure 6 shows the variation of the shear modulus G with the polymer weight fraction of the zwitterionic GSH. In Figure 6, at fixed polymer weight fraction C, G is larger in the glucose solution than in sugar-free PBS buffer, as might be expected if glucose-mediated reversible cross-linking is occurring (see Introduction). However, we also have the puzzling result that at fixed polymer weight fraction and at (presumably) fixed cross-link density, G is smaller in the fructose solution than in sugar-free PBS buffer. This might be an indication that the network chains are stiffer in the sugar-free PBS buffer than in the fructose solution. A similar result was observed for pH-responsive hydrogels in Reference 48.

One can use Equation (6) in conjunction with the shear modulus values of Figure 6 to perform a least-squares-fit on the measured values of Π_{tot}. The results of this fitting procedure are given by the continuous curves in Figure 5, and the fit is seen to be excellent. This fitting procedure provides values for the Flory-Huggins binary (χ_0) and ternary (χ_1) interaction parameters, which are shown in Figure 7 as obtained for the zwitterionic GSH in the fructose solution, in the glucose solution, and in sugar-free PBS buffer. All three χ_0 values are similar, but χ_1 is significantly larger in the glucose solution than in the fructose solution (0.51 vs. 0.43), with an intermediate value observed in sugar-free PBS buffer (0.46). From Equation (3), the larger value of χ_1 implies that Π_{mix}, which depends on thermodynamic mixing interactions rather than on cross-link density, is considerably less favorable for swelling in glucose solutions than in fructose solutions. This is consistent with the observation that the zwitterionic GSH shrinks in response to glucose (Figure 3), and swells in response to fructose (Figure 4).

4.3 Small-Angle Neutron Scattering Measurements

To obtain information on the spatial organization of the polymer molecules in these zwitterionic GSHs at the nanoscale, we made SANS measurements. Figure 8 shows the SANS spectra at 25 °C for the thermally-cured GSHs of Figures 3 and 4 swollen to the same extent (12 wt%) in three different solvents: sugar-free 1X PBS buffer, 1X PBS buffer plus 5 mM added glucose, and 1X PBS buffer plus 5 mM added fructose. Surprisingly, even though the swelling pressure of this GSH responds very differently to fructose and glucose (Figure 5 vs. Figure 6), the shape of the SANS spectra (Figure 8) is similar in fructose and glucose solutions. However, the scattering intensity from the gel swollen in glucose solution is greater than from the corresponding gel swollen in fructose solution by roughly a factor of two. The increase in intensity reflects a decrease in the osmotic modulus, which is consistent with the swelling pressure observations. Figure 9 shows the SANS response of a UV-cured GSH of the same nominal composition, as obtained after swelling to equilibrium in the same three solvents studied in Figure 8. Comparing Figures 8 and 9, one notes that the curing procedure (thermal vs. UV) has a little effect on the hydrogel structure in the low q (< 0.007 $Å^{-1}$) region, where the UV cured gel in glucose solution exhibits a slightly less steep negative slope.

The SANS curves were analyzed using equation (7), which reproduces the main characteristic features of the scattering curves

$$I(q)=\frac{A_1}{1+q^2\xi^2}+\frac{A_2}{q^s} \tag{7}$$

where ξ is the polymer-polymer correlation length [49], and A_1, A_2 and s are constants. The intensities A_1 and A_2 are proportional to the average scattering contrast between the polymer and the solvent. In equation (7) the first term (Lorentzian form factor) is primarily governed by the thermodynamic concentration fluctuations, while the second term arises from large-scale static inhomogeneities frozen-in by the cross-links. These large objects are not expected to make significant contribution to the thermodynamic properties of the system [50,51].

The parameters obtained from the least-squares fit of equation (7) to the SANS data (continuous lines in Figures 8 & 9) are listed in Table 1. The apparent invariance of ξ with the solvent composition suggests that glucose induced cross-linking does not affect appreciably the mesh size of these gels.

4.4 Temperature-dependent GSH Swelling Behavior in Fructose and Glucose Solutions

In section 4.2, it was shown that the thermodynamic interaction of the zwitterionic GSH is favorable with fructose and unfavorable with glucose (relative to sugar-free PBS buffer). In order to determine if this difference is enthalpic or entropic in origin, we compare the temperature-dependent swelling response of the GSH in 5 mM fructose solution, 5 mM glucose solution, and sugar-free PBS buffer (Figure 10). An increase in temperature is expected to favor processes that increase entropy relative to processes that reduce enthalpy. Figure 10 shows the change in the relative hydrogel swelling ratio in response to cyclic changes in temperature between 23 °C and 50 °C. The zwitterionic GSH in sugar-free PBS (1X) shrinks with increase in temperature; the shrinkage is slight (≈ 2%) but reproducible. This is typical behavior for many water-soluble polymers; it is thought to occur because the water molecules adopt a higher degree of order (lower entropy) near the polymer in order to maintain hydrogen bonding [52]. This structuring of water gives rise to the *hydrophobic interaction force* between polymer chains that is largely entropic in origin. When the GSH is placed in the fructose solution, thereby producing a polymer network containing adsorbed fructose molecules, the degree of hydrogel shrinkage is even larger (≈ 6%) with increase in temperature. In striking contrast, the GSH polymer network containing adsorbed glucose molecules is observed to swell with increase in temperature (Figure 10).

5. Discussion

The purpose of this study is to check the widely-held assumption [14,18,20–21,24,27,32], first proposed by Alexeev et al. [12], that the shrinkage of zwitterionic GSHs in response to an increase in glucose concentration arises almost entirely due to the formation of glucose mediated cross-links (i.e., $|\Delta\Pi_{el}| >> |\Delta\Pi_{mix}|$). Figure 5–7 contain the data needed to check this assumption. Consider an increase in environmental glucose concentration from 0 to 5 mM in PBS buffer, which clearly causes the zwitterionic GSH to shrink in the chemomechanical sensor (Figure 3). At a fixed polymer concentration in the GSH (C = 0.15), this increase in glucose concentration results in a decrease in total swelling pressure Π_{tot} of ≈ 20 kPa (Figure 5). According to Figure 6, the decrease in Π_{el} (increase in G) under the same conditions is approximately 3 kPa, thus $\Delta\Pi_{mix}$ is ≈ −17 kPa. In other words, when the glucose concentration is increased from zero to 5 mM, 85% of the thermodynamic driving force for the shrinkage of the zwitterionic GSH can be attributed to the decrease in

the favorability of thermodynamic mixing interactions, and 15% of the driving force can be attributed to the increase in shear modulus. Note that the sensor signal in Figure 3 is less than 20 kPa because the hydrogel volume shrinks to some extent within the sensor due to sensor compliance, as discussed in Reference 40.

It should be pointed out that the relative contributions of $\Delta\Pi_{el}$ and $\Delta\Pi_{mix}$ might be expected to differ when zwitterionic GSHs of much greater boronic acid content (30 mol.%) than studied here (8 mol.%) are subjected to large changes in environmental glucose concentration (0 – 40 mM), as in Reference 32. This may explain why the percentage increase in shear modulus due to the increase in glucose concentration reported in Reference 32 is much larger than reported here in Figure 6.

Since the difference between the degree of reversible cross-linking attributable to glucose and fructose is not great for our zwitterionic GSH, an alternate explanation must be found to explain the enhancement in glucose selectivity relative to fructose that is obtained by incorporating tertiary amines into the hydrogel. The results in Figure 10 provide a clue. In PBS buffer and in the fructose solution, the zwitterionic GSH shrinks with increase in temperature, as expected to occur when water molecules near the GSH are highly ordered in order to preserve a high degree of hydrogen bonding [52]. By contrast, the zwitterionic GSH swells with increase in temperature in the glucose solution. This suggests that the adsorption of glucose molecules by the hydrogel may affect the arrangement of neighboring water molecules in such a way that they do not have lower entropy than bulk water, and do not preserve a high degree of hydrogen bonding. Such a change in water structure would not be apparent in SANS spectra obtained from samples in heavy water. The loss in hydrogen bonding with increase in environmental glucose concentration is probably responsible for the decrease in the osmotic mixing pressure between the network and the solvent that causes the hydrogel to shrink.

6. Conclusions

Copolymerization of tertiary amines (Lewis bases) into glucose-responsive hydrogels containing boronic acid moieties creates a zwitterionic hydrogel with an enhanced selectivity for glucose relative to fructose, and also creates a hydrogel that shrinks rather than swells in response to an increase in environmental glucose concentration. Previously it had been thought that this occurs because glucose can mediate the formation of reversible cross-links in zwitterionic hydrogels, whereas fructose cannot. However, we have shown that another significant factor is the change in the value of Π_{mix}, which reflects the thermodynamic mixing interactions between the network and solvent. The zwitterionic GSH shrinks upon glucose addition and swells upon fructose addition because the change in Π_{mix} is large and negative in the first case, and large and positive in the second case.

Acknowledgments

This research was supported by the Intramural Research Program of the NICHD, NIH. We also acknowledge the support of the National Institute of Standards and Technology, U.S. Department of Commerce, in providing the neutron research facilities used in this work. This work utilized facilities supported in part by the National Science Foundation under Agreement No. DMR-0944772. This project was supported by the National Institutes of Health NHLBI/ NIBIB Grant # 5R21EB008571-02.

References

1. Koschinsky T, Heinemann L. Sensors for glucose monitoring: technical and clinical aspects. Diabetes Metab Res. Rev. 2001; 17:113–123. [PubMed: 11307176]

2. Koschwanez HE, Reichert WM. In vitro, in vivo and post explantation testing of glucose-detecting biosensors: Current methods and recommendations. Biomaterials. 2007; 28:3687–3703. [PubMed: 17524479]
3. Glindkamp A, Riechers D, Rehbock C, Hitzmann B, Scheper T, Reardon KE. Sensors in Disposable Bioreactors Status and Trends. Adv Biochem Engin/Biotechnol. 2009; 115:145–169.
4. Kurtinaitiene B, Razumiene J, Gureviciene V, Melvydas V, Marcinkeviciene L, Bachmatova I, Meskys R, Laurinavicius V. Application of oxygen-independent biosensor for testing yeast fermentation capacity. Biosensors & Bioelectronics. 2010; 26:766–771. [PubMed: 20673625]
5. Degani Y, Heller A. Direct electrical communication between chemically modified enzymes and metal electrodes.1. Electron transfer from glucose oxidase to metal electrodes via electron relays, bound covalently to the enzyme. J. Phys. Chem. 1987; 91:1285–1289.
6. Degani Y, Heller A. Direct electrical communication between chemically modified enzymes and metal electrodes. 2. Methods for bonding electron-transfer relays to glucose oxidase and D-amino-acid oxidase. J. Amer. Chem. Soc. 1988; 110:2615–2620.
7. Kudo H, Sawada T, Kazawa E, Yoshida H, Iwasaki Y, Mitsubayahi K. A flexible and wearable glucose sensor based on functional polymers with Soft-MEMS techniques. Biosensors & Bioelectronics. 2006; 22:558–562. [PubMed: 16777401]
8. Gough DA, Kumosa LS, Routh TL, Lin JT, Lucisano JY. Function of an Implanted Tissue Glucose Sensor for More than 1 Year in Animals. Sci. Traslational Med. 2010; 2:42–53.
9. Jiang X, Wu Y, Mao X, Cui X, Zhu L. Amperometric glucose biosensor based on integration of glucose oxidase with platinum nanoparticles/ordered mesoporous carbon nanocomposite. Sensors & Actuators, B, Chem. 2011; 153:158–163.
10. Arnold FH, Zheng W, Michaels AS. A membrane-moderated conductimetric sensor for the detection and measurement of specific organic solutes in aqueous solutions. J. Membrane Sci. 2000; 167:227–239.
11. Asher SA, Alexeev VL, Goponenko AV, Sharma AC, Lednev IK, Wilcox CS, Finegold DN. Photonic Crystal Carbohydrate Sensors: Low Ionic Strength Sugar Sensing. J. Am. Chem. Soc. 2003; 125:3322–3329. [PubMed: 12630888]
12. Alexeev VL, Sharma AC, Goponenko AV, Das S, Lednev IK, Wilcox CS, Finegold DN, Asher SA. High ionic strength glucose-sensing photonic crystal. Analytical Chem. 2003; 75:2316–2323.
13. Lee Y-J, Pruzinsky SA, Braun PV. Glucose-Sensitive Inverse Opal Hydrogels: Analysis of Optical Diffraction Response. Langmuir. 2004; 20:3096–3106. [PubMed: 15875835]
14. Horgan AM, Marshall AJ, Kew SJ, Dean KES, Creasey CD, Kabilan S. Crosslinking of phenylboronic acid receptors as a means of glucose selective holographic detection. Biosensors & Bioelectronics. 2006; 21:1838–1845. [PubMed: 16414255]
15. Samoei GK, Wang W, Escobedo JO, Xu X, Schneider H-J, Cook RL, Strongin RM. A Chemomechanical Polymer that Functions in Blood Plasma with High Glucose Selectivity. Angew. Chem. Int. Ed. 2006; 45:5319–5322.
16. Yang X, Lee M-C, Sartain F, Pan X, Lowe CR. Designed Boronate Ligands for Glucose-Selective Holographic Sensors. Chem. Eur. J. 2006; 12:8491–8497. [PubMed: 16906615]
17. Lei M, Baldi A, Nuxoll E, Siegel RA, Ziaie B. A Hydrogel-Based Implantable Micromachined Transponder for Wireless Glucose Measurement. Diabetes Technology & Therapeutics. 2006; 8:112–122. [PubMed: 16472058]
18. Yang X, Pan X, Blyth J, Lowe CR. Towards the real-time monitoring of glucose in tear fluid: Holographic glucose sensors with reduced interference from lactate and pH. Biosens. Bioelect. 2008; 23:899–905.
19. Kuzimenkova MV, Ivanov AE, Thammakhet C, Mikhalovska LI, Galaev IY, Thavarungkul P, Kanatharana P, Mattiasson B. Optical Responses, permeability and diol-specific reactivity of thin polyacrylamide gels containing immobilized phenylboronic acid. Polymer. 2008; 49:1444–1454.
20. Tierney S, Volden S, Stokke BT. Glucose sensors based on a responsive gel incorporated as a Fabry-Perot cavity on a fiber-optic readout platform. Biosens. Bioelectron. 2009; 24:2034–2039. [PubMed: 19062267]

21. Tierney S, Falch BMH, Hjelme DR, Stokke BT. Determination of Glucose Levels Using a Functionalized Hydrogel-Optical Fiber Biosensor: Toward Continuous Monitoring of Blood Glucose in Vivo. Anal. Chem. 2009; 81:3630–3636. [PubMed: 19323502]
22. Huang X, Li S, Schultz JS, Wang Q, Lin Q. A MEMS affinity glucose sensor using a biocompatible glucose-responsive polymer. Sens. Actuators, B, Chem. 2009; 140:603–609.
23. Torun O, Dudak FC, Bas D, Tamer U, Boyaci IH. Thermodynamic analysis of the interaction between 3-aminophenylboronic acid and monosaccharides for development of biosensor. Sensors & Actuators, B, Chem. 2009; 140:597–602.
24. Lin G, Chang S, Hao H, Tathireddy P, Orthner M, Magda J, Solzbacher F. Osmotic Swelling Pressure Response of Smart Hydrogels Suitable for Chronically-Implantable Glucose Sensors. Sensors & Actuators, B, Chem. 2010; 144:332–336.
25. Badugu R, Lakowicz JR, Geddes CD. Ophthalmic glucose sensing: a novel monosaccharide sensing disposable and colorless contact lens. Analyst. 2001; 129:516–521. [PubMed: 15152329]
26. Suri JT, Cordes DB, Cappuccio FE, Wessling RA, Singaram B. Continuous Glucose Sensing with a Fluorescent Thin-Film Hydrogel. Angew. Chem. Int. Ed. 2003; 42:5857–5859.
27. Dean KES, Horgan AM, Marshall AJ, Kabilan S, Pritchard J. Selective holographic detection of glucose using tertiary amines. Chem. Commun. 2006:3507–3509.
28. Yan J, Fang H, Wang B. Boronolectins and Fluorescent Boronolectins: An Examination of the Detailed Chemistry Issues Important for the Design. Medicinal Research Reviews. 2005; 25:490–520. [PubMed: 16025498]
29. Kataoka K, Miyazaki H, Bunya M, Okano T, Sakurai Y. Totally Synthetic Polymer Gels Responding to External Glucose Concentration: Their Preparation and Application in On-Off Regulation of Insulin Release. J. Am. Chem. Soc. 1998; 120:12694–12695.
30. Kitano S, Hisamitsu I, Koyama Y, Kataoka K, Okano T, Sakurai Y. Effect of the Incorporation of Amino Groups in a Glucose-responsive Polymer Complex Having Phenylboronic Acid Moieties. Polymers for Adv. Technologies. 1991; 2:261–264.
31. Kawasaki TH, Akanuma H, Yamanouchi T. Increased Fructose Concentrations in Blood and Urine in Patients with Diabetes. Diabetes Care. 2002; 25:353–357. [PubMed: 11815509]
32. Mujumdar, SK. PhD Thesis. University of Minnesota; 2008.
33. Hisamitsu I, Kataoka K, Okano T, Sakurai Y. Glucose-Responsive Gel from Phenylborate Polymer and Poly(Vinyl Alcohol): Prompt Response at Physiological pH Through the Interaction of Borate with Amino Group in the Gel. Pharmaceutical Research. 1997; 14:289–293. [PubMed: 9098868]
34. Flory, PJ. Principles of Polymer Chemistry. Ithaca, New York: Cornell University Press; 1953.
35. Dusek K, Prins W. Structure and elasticity of non-crystalline polymer networks. Adv. Poly. Sci. 1969; 6:1–102.
36. Horkay F, Tasaki I, Basser PJ. Osmotic Swelling of Polyacrylate Hydrogels in Physiological Salt Solutions. Biomacromolecules. 2000; 1:84–90. [PubMed: 11709847]
37. Horkay F, Basser PJ. Osmotic observations on chemically cross-linked DNA gels in physiological salt solutions. Biomacromolecules. 2004; 5:232–237. [PubMed: 14715031]
38. Yin DW, Horkay F, Douglas JF, De Pablo JJ. Molecular simulation of the swelling of polyelectrolyte gels by monovalent and divalent counterions. J. Chem. Phys. 2008; 129(15) art. no. 154902.
39. Han IS, Han M-H, Kim J, Lew S, Lee YJ, Horkay F, Magda JJ. Constant-Volume Hydrogel Osmometer: A New Device Concept for Miniature Biosensors. Biomacromolecules. 2002; 3:1271–1275. [PubMed: 12425665]
40. Lin G, Chang S, Kuo C-H, Magda J, Solzbacher F. Free Swelling and Confined Smart Hydrogels for Applications in Chemomechanical Sensors for Physiological Monitoring. Sens. Actuators, B, Chem. 2009; 136:186–195. [PubMed: 20130753]
41. Vink H. Precision measurements of osmotic pressure in concentrated polymer solutions. Eur. Polym. J. 1971; 7:1411–1419.
42. Brown, RP. Physical Testing of Rubber. 2nd ed. New York: Elsevier; 1986.
43. Mooney M. The Thermodynamics of a Strained Elastomer. I. General Analysis. J. Appl. Phys. 1948; 19:434–444.

44. Rivlin RS. Torsion of a Rubber Cylinder. J. Appl. Phys. 1947; 18:444–449.

45. NIST Cold Neutron Research Facility. NG3 and NG7 30-meter SANS Instruments Data Acquisition Manual. 1999 January.

46. Horkay F, Hecht AM, Mallam S, Geissler E, Rennie AR. Macroscopic and microscopic thermodynamic observations in swollen poly(vinyl acetate) networks. Macromolecules. 1991; 24:2896–2902.

47. Tathireddy, P.; Avula, M.; Lin, G.; Cho, S-H.; Guenther, M.; Schulz, V.; Gerlach, G.; Magda, J.; Solzbacher, F. Smart Hydrogel Based Microsensing Platform for Continuous Glucose Monitoring. IEEE Engineering in Medicine and Biology Conference (EMBC) 2010, Buenos Aires; Aug 31 – Sep 3, 2010; Argentina.

48. Horkay F, Han M-H, Han IS, Bang I-S, Magda JJ. Separation of the effects of pH and polymer concentration on the swelling pressure and elastic modulus of a pH-responsive hydrogel. Polymer. 2006; 47:7335–7338. [PubMed: 17917687]

49. de Gennes, P-G. Scaling Concepts in Polymer Physics. Ithaca, NY: Cornell; 1979.

50. Horkay F, Hecht AM, Geissler E. Fine structure of polymer networks as revealed by solvent swelling. Macromolecules. 1998; 31:8851–8856.

51. Horkay F, McKenna GB, Deschamps P, Geissler E. Neutron scattering properties of randomly cross-linked polyisoprene gels. Macromolecules. 2000; 33:5215–5220.

52. Prausnitz, JM.; Lichtenhaler, RN.; de Azevedo, EG. Molecular Thermodynamics of Fluid-Phase Equilibria. 3rd Ed. New Jersey: Prentice Hall, Upper Saddle River; 1999. p. 94-96.

Biographies

Ferenc Horkay received his PhD in Chemistry (1978) from the Loránd Eötvos University (Budapest) and DSc from the Hungarian Academy of Sciences. Prior to joining the National Institutes of Health in 1999, he was a senior research scientist at the Corporate Research and Development Center of the General Electric Corporation (Schenectady, NY). His research interest is to understand the fundamental principles that govern molecular interactions and define structural hierarchy in complex synthetic and biopolymer systems, such as gels, self-assemblies and functional nanostructures. Since 2010 he is the Chair of the Polymer Networks Group, a worldwide organization of polymer physicists, chemists, biologists, materials scientists and engineers.

Seung Hei Cho is a graduate student in Chemical Engineering at the University of Utah. She received a B.S. degree in Chemical Engineering in 2004 from Hanyang University, and a M.S. degree in Chemical Engineering in 2006 from Hanyang University. Her research area is synthesis and testing of stimuli-responsive hydrogels.

Prashant Tathireddy received a bachelor's degree in Chemical Technology from the Osmania University, Hyderabad, India in 1997. He was a project leader at Computer Maintenance Corporation Private Limited, Hyderabad, India till 1999. He received a PhD degree in Chemical Engineering in June 2005 from University of Utah. He later joined the Microsystems Laboratory at the University of Utah as a post doctoral fellow and worked in that position till 2007. He received a Fraunhofer fellowship award in 2007 and was posted as a guest scientist at the Fraunhofer Institute for Biomedical Engineering (IBMT), St. Ingbert, Germany. He currently holds a position as research assistant professor in the department of Electrical & Computer Engineering at Utah. He has previously contributed to disciplines such as microfluidics and material characterization using impedance spectroscopy while his current research focuses on design, fabrication process development and testing of implantable medical microdevices or BioMEMs. This includes design and development of electronic packaging and new encapsulation techniques of medical devices for chronic use.

Loren Rieth received his BS degree in materials science from The Johns-Hopkins University, Baltimore, MD, in 1994. He received his PhD in materials science and engineering from the University of Florida, Gainesville, FL, in 2001. From 2001 to 2003, he was a postdoctoral research associate at the University of Utah, Salt Lake City, UT, and continued on at the University of Utah as a research assistant professor in materials science (2003–2005), and electrical and computer engineering (2004–present). His research is focused on deposition and characterization of thin film materials for sensors (chemical, physical, and biological), MEMS, BioMEMS, and energy production.

Florian Solzbacher is Director of the Microsystems Laboratory at the University of Utah and an Associate Professor in Electrical and Computer Engineering with adjunct appointments in Materials Science and Bioengineering. His research focuses on harsh environment microsystems and materials, including implantable, wireless microsystems but also high temperature and harsh environment compatible micro sensors. Prof. Solzbacher received his M.Sc. EE from the Technical University Berlin in 1997 and his Ph.D. from the Technical University Ilmenau in 2003. He is co-founder of several companies such as I2S Micro Implantable Systems, First Sensor Technology and NFocus. He is Chairman of the German Association for Sensor Technology AMA, and serves on a number of company and public private partnership advisory boards. He is author of over 100 journal and conference publications, 5 book chapters and 13 pending patents.

Jules Magda is a Professor in Chemical Engineering and in Materials Science & Engineering at the University of Utah. He received his BS in chemical engineering in 1979 from Stanford University, and his PhD in chemical engineering and materials science in 1986 from the University of Minnesota in Minneapolis. His areas of interest include stimuli-responsive hydrogels and biomedical sensors for treatment of diabetes and obesity.

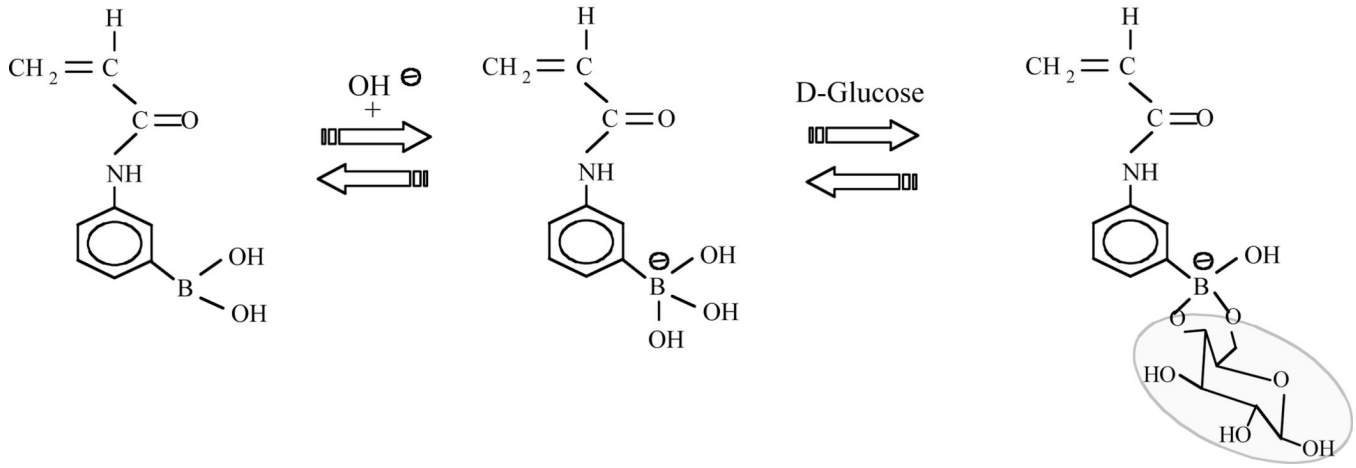

Figure 1.
From left-to-right, the interaction between the boronic acid moiety (on acrylamide monomer) and a hydroxyl group to form the charged boronate moiety; reversible binding between the boronate moiety and a diol such as on D-glucose to form a cyclic boronic acid ester (tridentate binding is also possible).

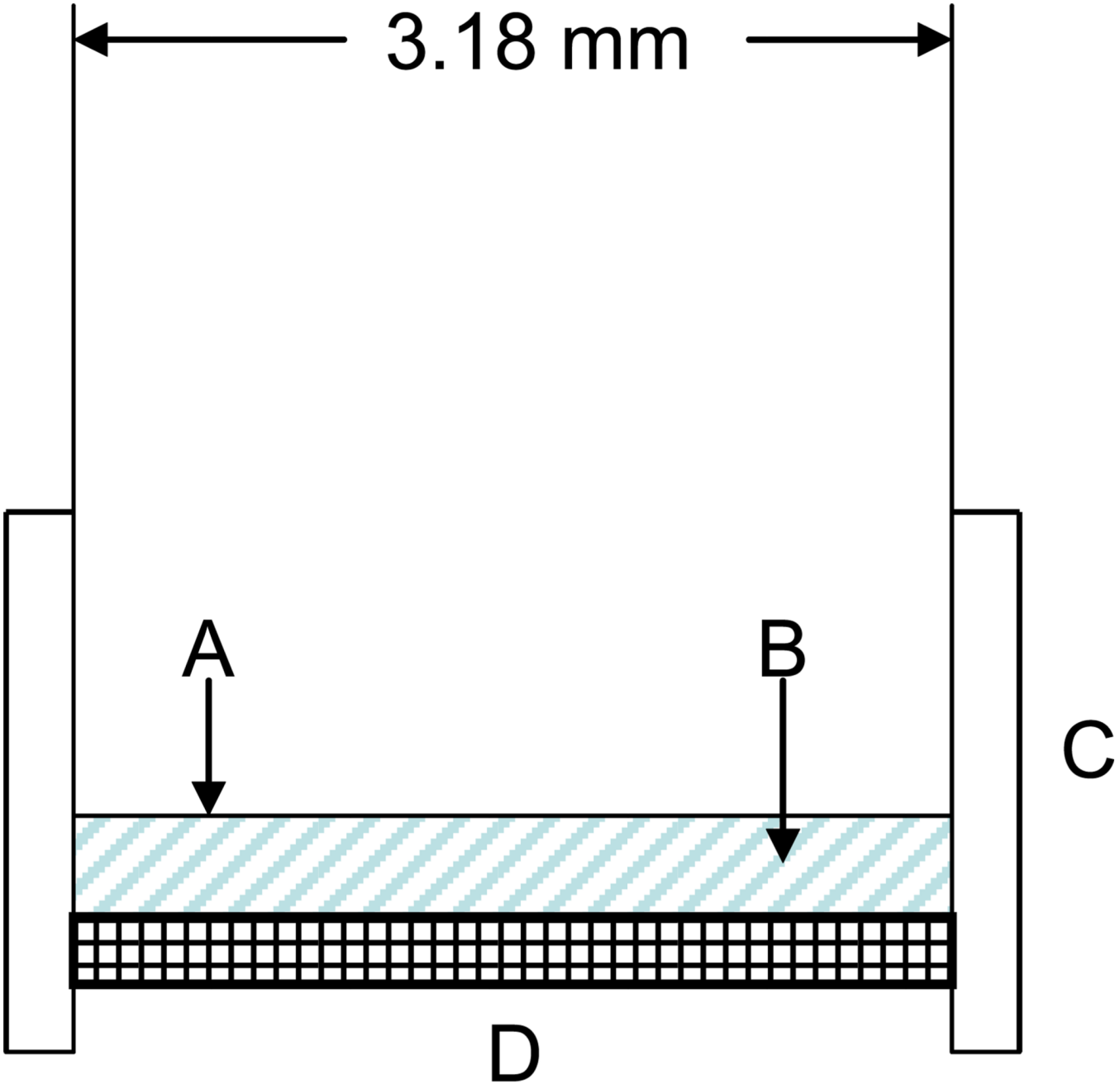

Figure 2.
Preliminary version of the chemomechanical sensor used in this study. A piezoresistive pressure transducer with a cylindrical sensing area (A) is completely covered with a disc-shaped hydrogel film (B) of approximate thickness 400 microns. The hydrogel is held in place by a cap (C) that has a top surface which is a replaceable wire mesh/porous membrane (D) (from Reference 40).

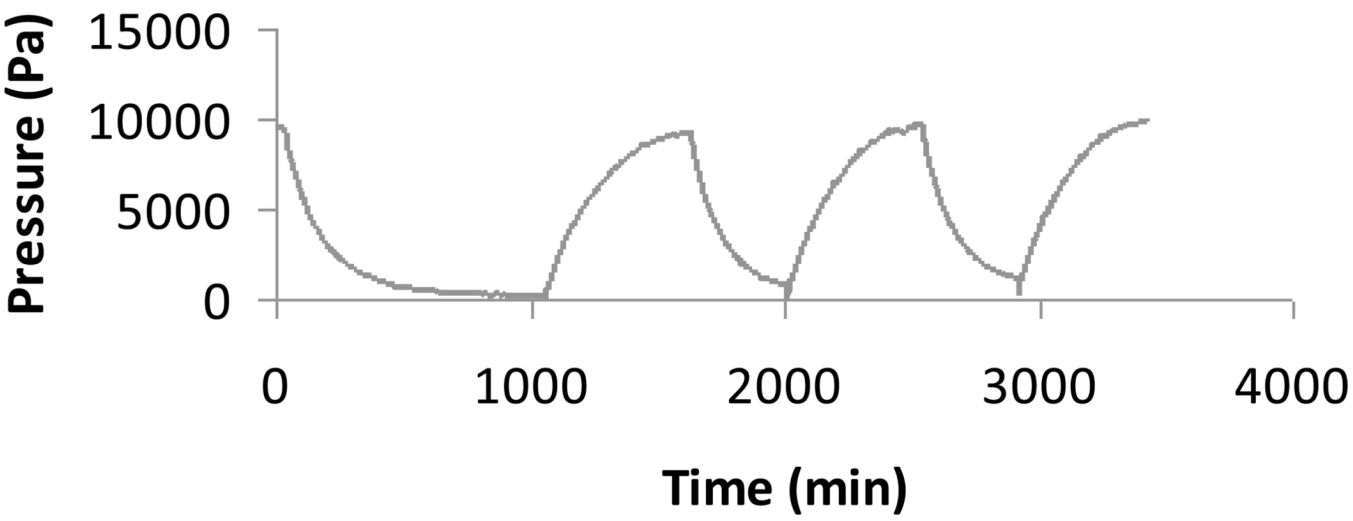

Figure 3.
Time-dependent change in pressure relative to baseline measured by chemomechanical sensor of Figure 2 in response to cyclic change in glucose at fixed pH 7.4 and fixed ionic strength 0.16 M in 1X PBS buffer. The environmental glucose concentration, which was initially zero, was suddenly increased to 5 mM at time equal zero, suddenly reduced to zero again at time equal 1100 minutes, and then the cycle was repeated twice more (thermally-cured zwitterionic GSH, pre-gel polymer concentration 13 wt.%).

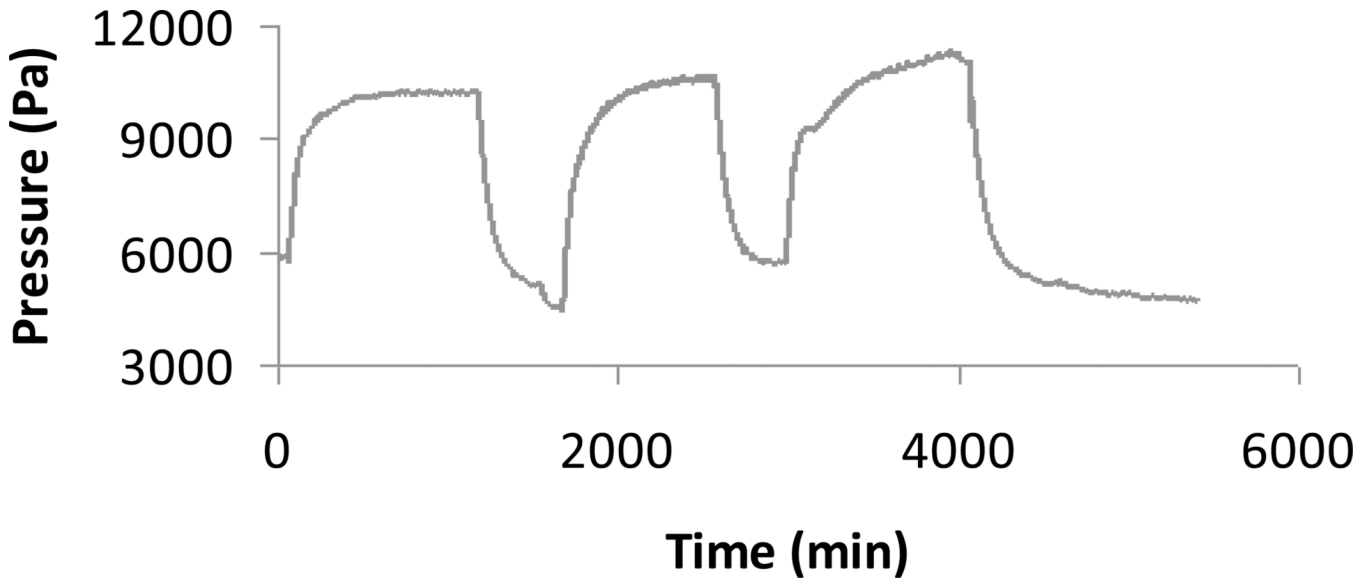

Figure 4.
Time-dependent change in pressure relative to baseline measured by chemomechanical sensor of Figure 2 in response to cyclic change in fructose at fixed pH 7.4 and fixed ionic strength 0.16 M in 1X PBS buffer. The environmental fructose concentration, which was initially zero, was suddenly increased to 5 mM at time equal zero, suddenly reduced to zero again at time equal 1100 minutes, and then the cycle was repeated twice more (thermally-cured zwitterionic GSH, pre-gel polymer concentration 13 wt.%).

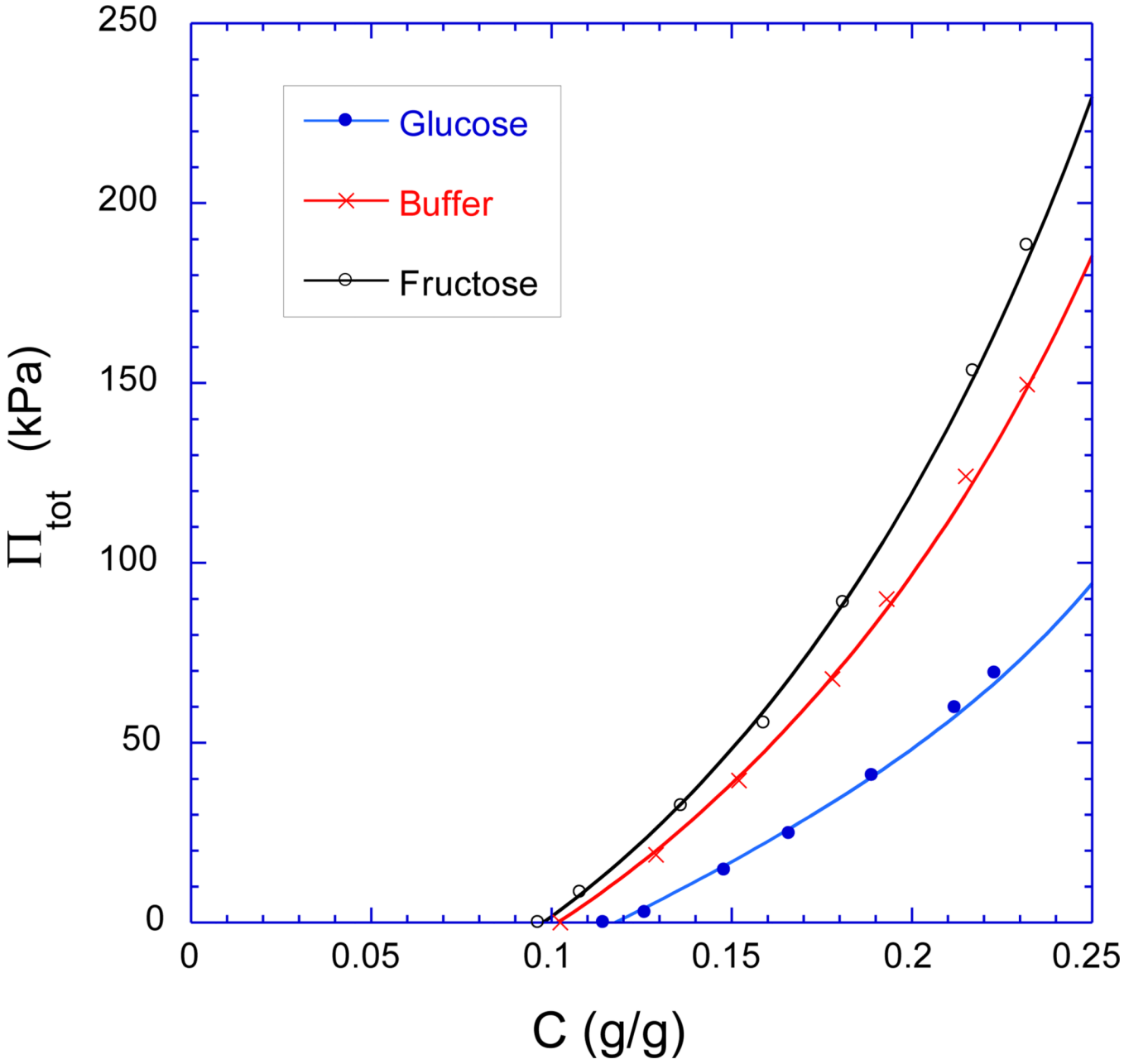

Figure 5.
Total osmotic swelling pressure vs. polymer weight fraction C for thermally-cured zwitterionic GSHs at 25 °C in sugar-free 1X PBS buffer (pH 7.4, 0.16 M ionic strength), PBS buffer with 5.0 mM added glucose, and PBS buffer with 5.0 mM added fructose. The continuous curves are least squares fits to Equation (6) in the text (pregel polymer concentration 13 wt.%).

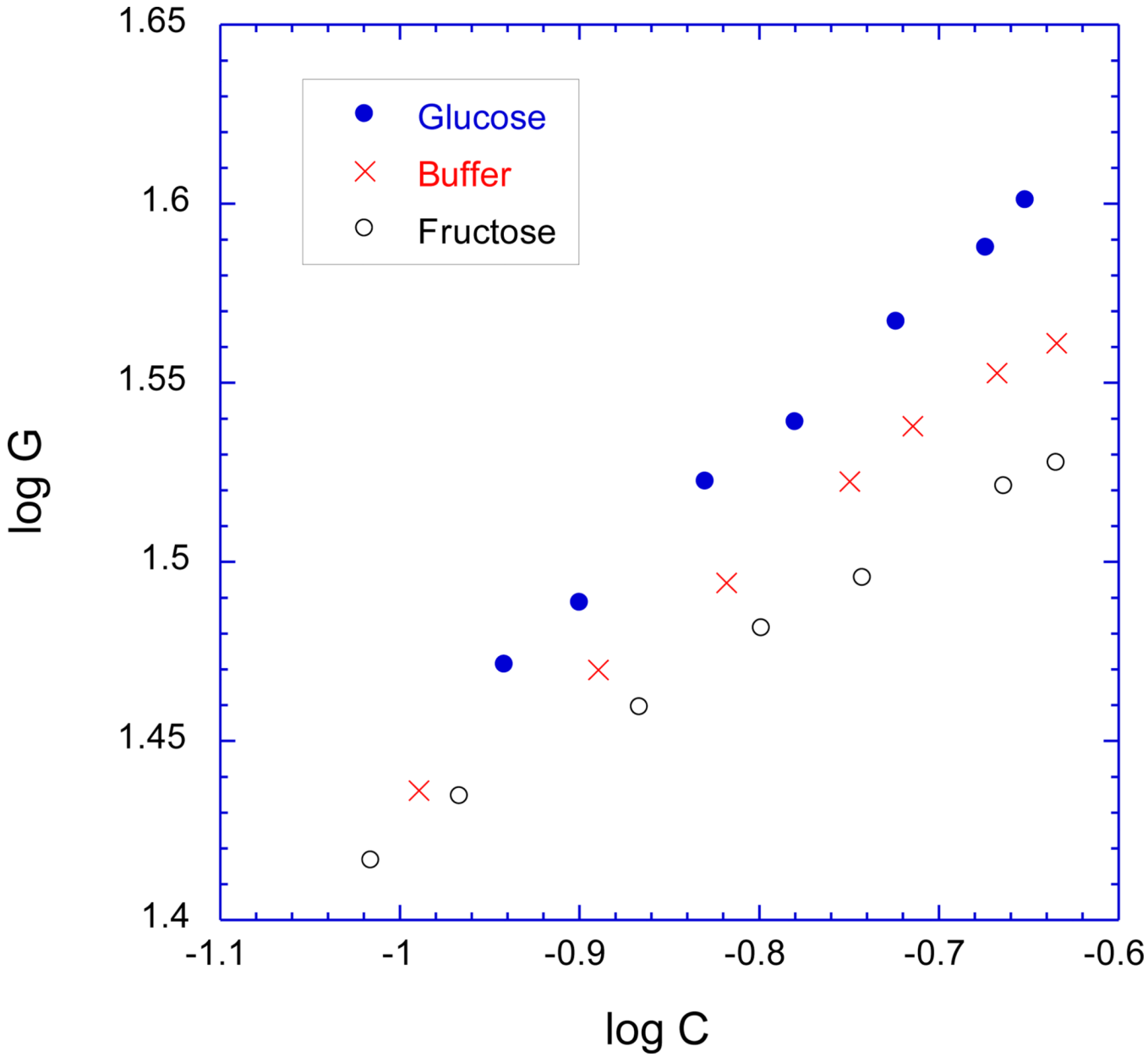

Figure 6.
Logarithmic plot of elastic shear modulus G (in kPa) vs. polymer weight fraction C, as measured in the three different solutions studied in Fig.5 (thermally-cured zwitterionic GSH, pre-gel polymer concentration 13 wt.%).

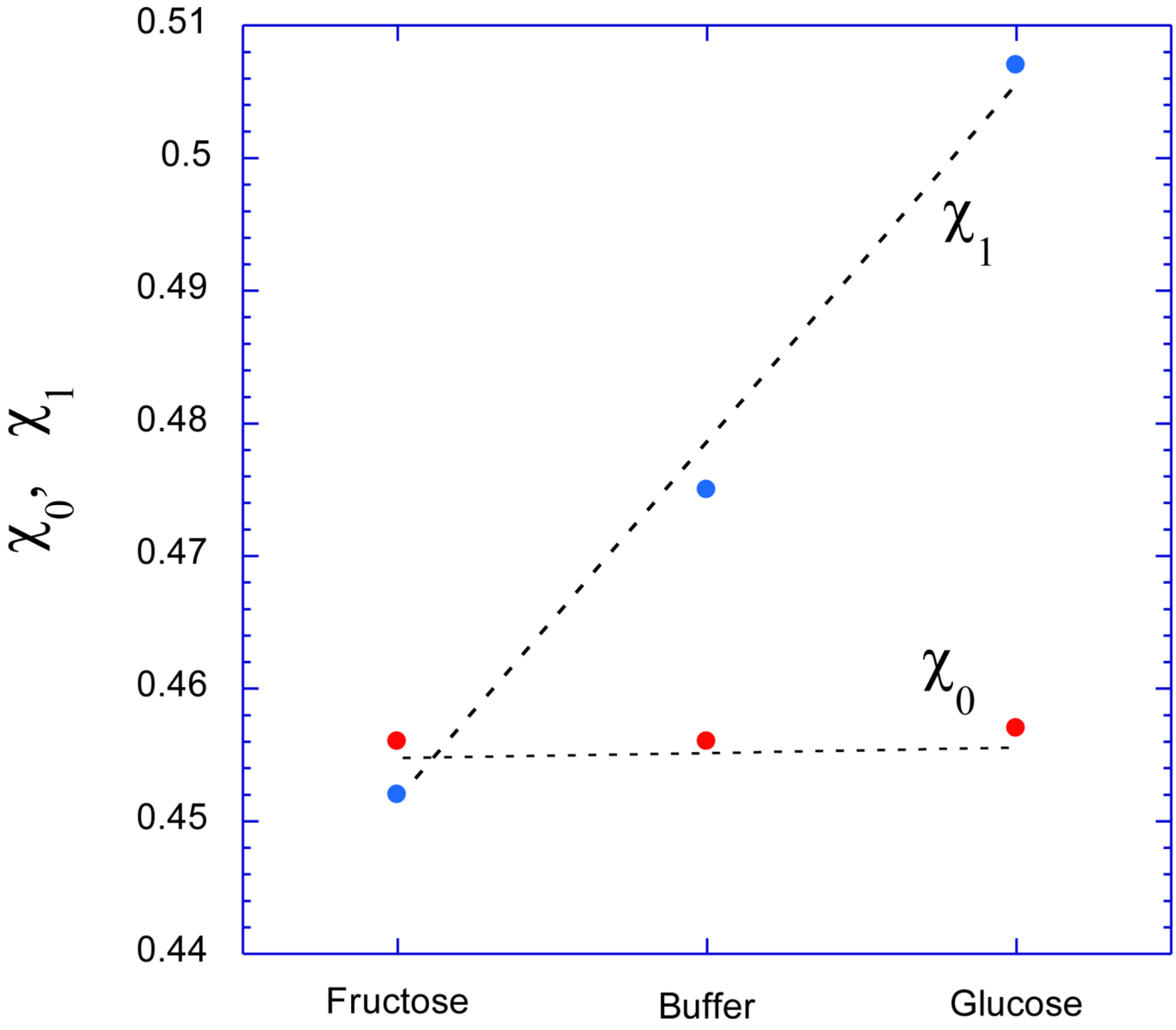

Figure 7.
Values of the Flory-Huggins binary and ternary interaction parameters as obtained by least-squares-fit of the data in Figure 5 to Equation (6). The broken lines through the data points serve as guides to the eyes.

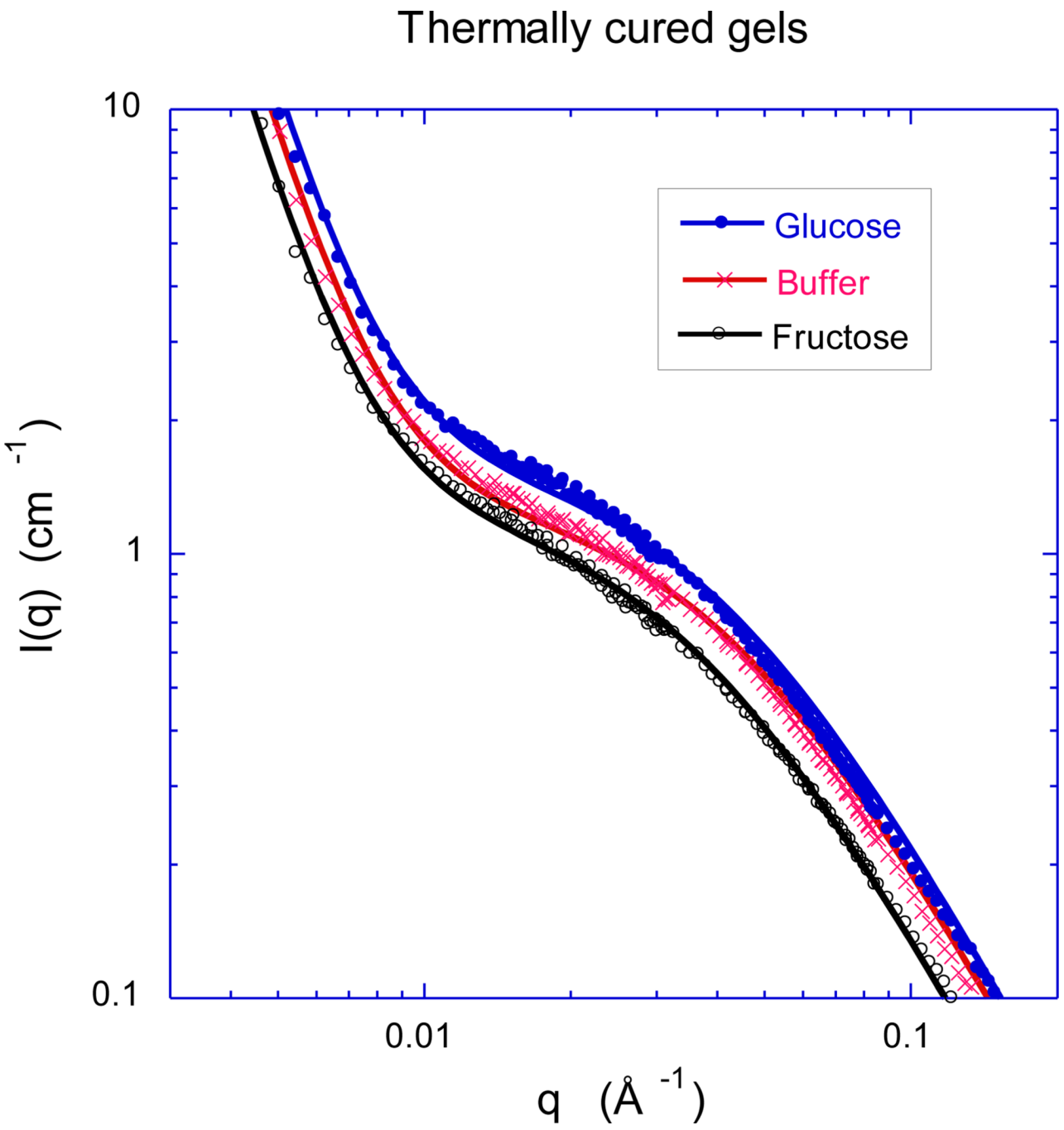

Figure 8.
Comparison of SANS spectra obtained from zwitterionic GSHs at 25 °C in sugar-free 1X PBS buffer (pH 7.4, 0.16 M ionic strength), PBS buffer with 5.0 mM added glucose, and PBS buffer with 5.0 mM added fructose. The GSHs were obtained by thermal curing of a pre-gel solution containing 13.0 wt.% polymer. The continuous curves are least squares fits of Equation (7) to the data.

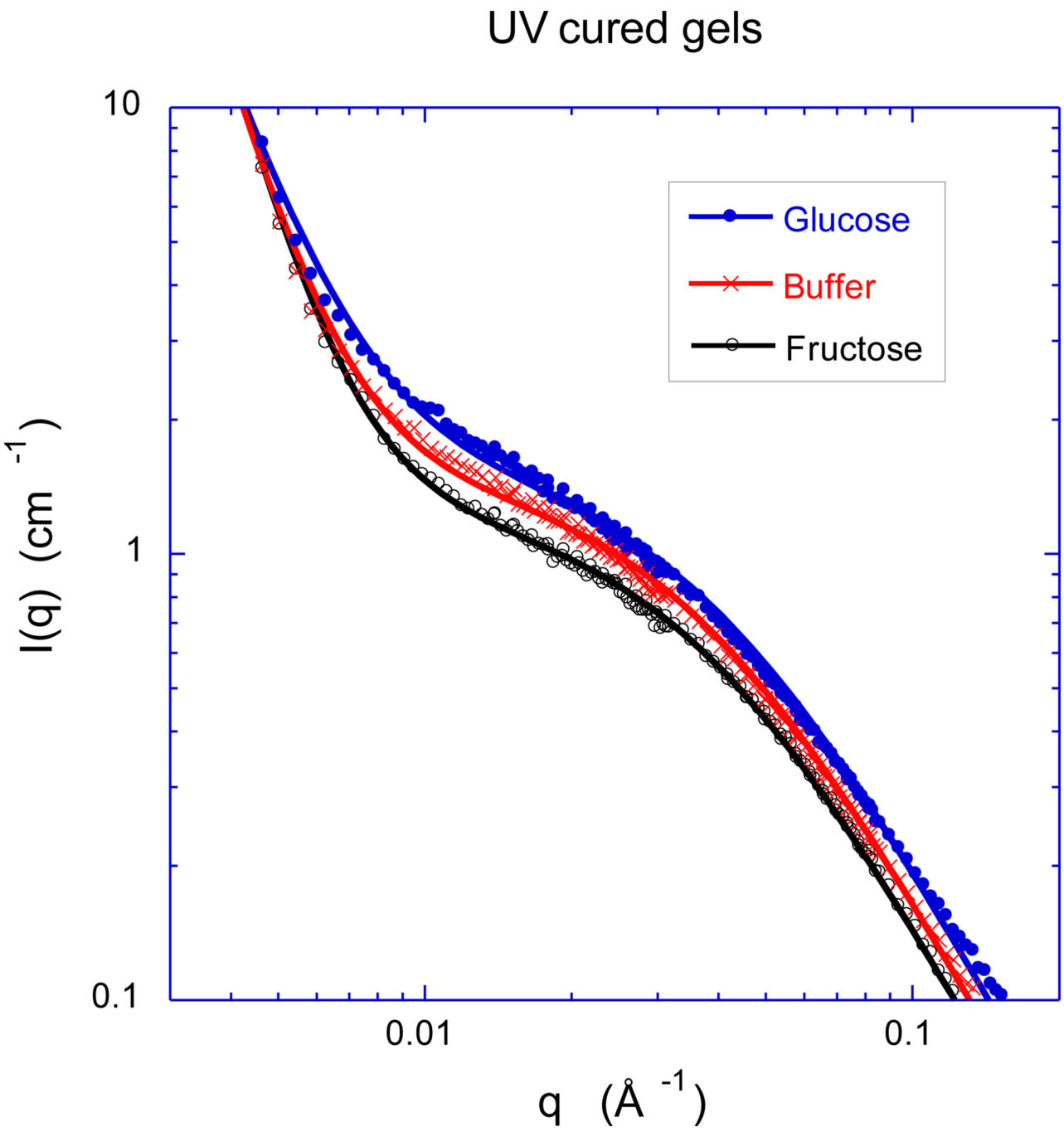

Figure 9.
Comparison of SANS spectra obtained from zwitterionic GSHs at 25 °C in sugar-free 1X PBS buffer (pH 7.4, 0.16 M ionic strength), PBS buffer with 5.0 mM added glucose, and PBS buffer with 5.0 mM added fructose. The GSHs were obtained by UV curing of a pre-gel solution containing 13.0 wt.% polymer. The continuous curves are least squares fits of Equation (7) to the data.

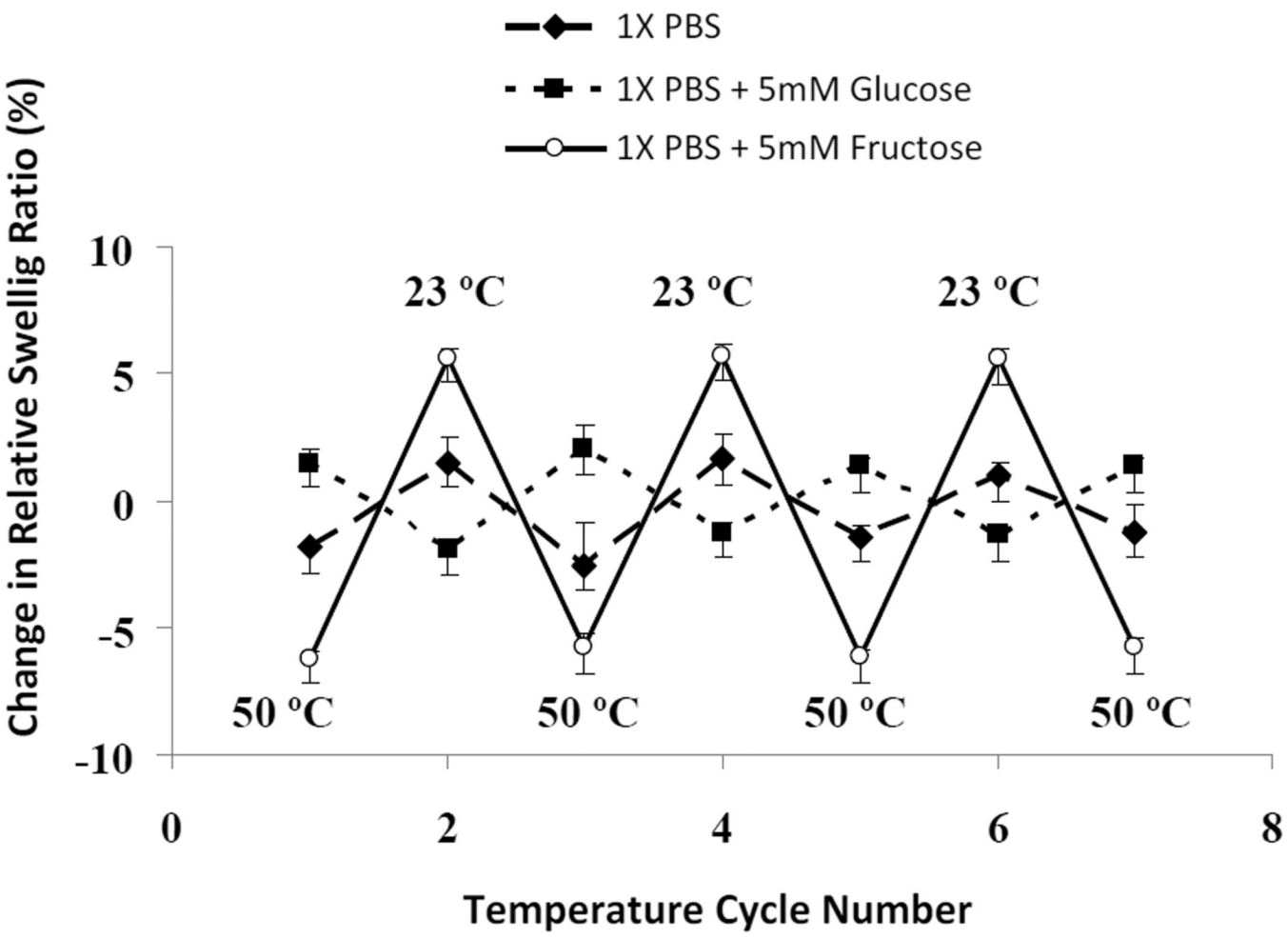

Figure 10.
Response of the relative swelling ratio to cyclic changes in temperature between 50 °C and 23 °C in the solvents given in the legend (UV-cured zwitterionic GSH, pre-gel polymer concentration 20 wt.%).

Table 1

Parameters from fits of equation 7 to the SANS spectra of thermal cured and UV cured gels

Sample	A_1 (cm^{-1})	A_2 (cm^{-1})	ξ (Å)	*s*
T/Glucose	0.009 ± 0.002	1.58 ± 0.4	25 ± 3	−3.77
T/Buffer	0.009 ± 0.002	1.29 ± 0.3	24 ± 3	−3.76
T/Fructose	0.008 ± 0.002	1.24 ± 0.3	23 ± 4	−3.78
UV/Glucose	0.008 ± 0.002	1.56 ± 0.5	26 ± 4	−3.35
UV/Buffer	0.007 ± 0.002	1.46 ± 0.4	27 ± 4	−3.74
UV/Fructose	0.007 ± 0.002	1.24 ± 0.3	28 ± 5	−3.91